# DESCRIBING THE MECHANOSENSITIVE ROLE OF AFFERENT RENAL NERVE ACTIVITY RELATED TO ARTERIAL PRESSURE

by

Christian Leung



A Thesis Submitted to the Faculty of the

DEPARTMENT OF BIOMEDICAL ENGINEERING

In Partial Fulfillment of the Requirements

For the Degree of

MASTER OF SCIENCE

In the Graduate College

THE UNIVERSITY OF ARIZONA

2023

2

THE UNIVERSITY OF ARIZONA
GRADUATE COLLEGE

As members of the Master's Committee, we certify that we have read the thesis prepared by *Christian Hubert Leung*, titled *Describing the Mechanosensitive Behavior of Afferent Renal Nerve Activity* and recommend that it be accepted as fulfilling the thesis requirement for the Master's Degree.

*Christopher T Banek, PhD* Date: May 3, 2023

*Jean-Marc Fellous*
Jean-Marc Fellous (May 3, 2023 10:03 PDT)
*Jean-Marc Fellous, PhD* Date: May 3, 2023

*Andrew J Fuglevand, PhD* Date: May 3, 2023

Final approval and acceptance of this thesis is contingent upon the candidate's submission of the final copies of the thesis to the Graduate College.

We hereby certify that we have read this thesis prepared under our direction and recommend that it be accepted as fulfilling the Master's requirement.

*Christopher T Banek, PhD* Date: May 3, 2023
Master's Thesis Committee Co-Chair
*Physiology*

*Jean-Marc Fellous*
Jean-Marc Fellous (May 3, 2023 10:03 PDT)
*Jean-Marc Fellous, PhD* Date: May 3, 2023
Master's Thesis Committee Co-Chair
*Biomedical Engineering*

**Table of Contents**

Abstract

Afferent renal nerves reportedly have an influential role in cardiovascular homeostasis – in health and disease. While the effects of afferent renal nerve manipulation have been studied, particularly in the scope of renal nerve ablation, the underlying neural mechanism contributing to cardiovascular regulation remains unclear. The goal of this study is to identify the relationship between afferent renal nerve activity and arterial pressure changes in the kidney, in both healthy and deoxycorticosterone acetate (DOCA) salt rat model of hypertension (high blood pressure). Male Sprague-Dawley Rats (275–300 g) were divided into normotensive (healthy) (n=5) and hypertensive DOCA groups (n=3). The DOCA group were administered 100mg DOCA subcutaneously and 0.9% saline drinking water for 21 days. Multiunit, extracellular afferent renal nerve activity (ARNA) recordings were conducted under urethane anesthesia (1800 mg/kg/h, IV) at protocol end. Afferent renal spikes were extracted on Spike2 and correlated with systolic and diastolic pressure peaks from the arterial pressure trace. For healthy animals, we detected a significant increase in afferent renal nerve spiking at diastole (0.28 spikes per 10ms/total heartbeats ± 0.13 in the time bin 10-0 milliseconds before diastole, Dunnett's Multiple Comparisons) when compared to each individual animal's baseline spike rate. In the hypertensive group, we failed to detect elevated rate at systole or diastole but saw significant activity around each stimulus (0.53 spikes per 10ms/total heartbeats ± 0.24 at 40-30 milliseconds before diastole and 0.49 s spikes per 10ms/total heartbeats ± 0.34 at 20-30 milliseconds after diastole, Dunnett's Multiple Comparisons). These results suggest that renal afferent spike train

temporal structure in healthy animals relies on arterial pressure change while hypertensive DOCA animals have a peak spiking activity temporal shift, as well as a lower relative activation compared to healthy animals, possibly explaining the destruction of ARNA modulation of cardiac control in DOCA salt hypertension at the site of the kidney.

## Introduction

Renal contributions to cardiovascular disease (CVD) have sparked efforts to understand the exact effects as well as mechanisms of renal dysfunction and the relationship to the heart, one of the most important factors being hypertension (Matsushita, et al., 2022). By looking at the site of renal nerves, major efforts have been devoted to studying neural control, particularly through looking at the effects of renal nerve ablation due to its effects on blood pressure (Katsurada et al., 2022). Renal nerve ablation has been seen to lower blood pressure in short- and long-term effects of patients (Ott et al., 2022), showing control of sympathetic and sensory renal nerves in this control.

Renal sympathetic nerves have a multitude of understood functions that affect the cardiovascular system including innervation of renal blood flow, control of sodium and water control, and release of renin (Sata et al., 2018). In Osborne, 2018 review, renal sympathetic nerves receive input from intermediolateral cell column in the spinal cord where pathways in the brain include the rostral ventrolateral medulla (RVLM) of the brainstem and paraventricular nucleus (PVN) of the hypothalamus. Both areas are known for autonomic control, especially in cardiac control and modulation (Nishi, et al., 2017). Elimination of this signal through sympathetic nerve ablation can explain how blood pressure is reduced in patients.

In light of renal sympathetic role understanding, the role of afferent renal nerves has been highlighted in recent studies with additional evidence of cardiac control. in Kopp et al., 2007, the modulation of afferent renal nerves by norepinephrine at the site of alpha 1 and 2 adrenergic

receptors in the pelvic wall were outlined. The term renorenal reflex, coined by the Kopp group, described the modulation of RSNA by afferent firing. In this argument, diseased states would be expected to demonstrate increased afferent spiking to combat vasoconstriction caused by sympathetic nerves. This work links sympathetic roles, most interestingly cardiovascular control, with sensory feedback.

However, interestingly in Banek, 2016 work on DOCA salt rats, elevated levels of ARNA in hypertensive groups compared to sham demonstrated evidence of renal afferent contribution in a diseased model dissented the work by the Kopp group. Afferent nerve ablation in this study also notably yielded a significant attenuation of blood pressure compared to sham animals as well. Afferent renal nerve activity is less understood, in part because of how sympathetic bursts conceal sensory nerve spiking during an in vivo recording. Understanding the specific role of sympathetic versus sensory input control will be essential in understanding the pathway and mechanism of neural control of cardiovascular control.

To unveil the mechanism of ARNA control, our group decided to analyze afferent renal nerve spiking with the hopes of understanding when spiking occurs in relation to arterial pressure in healthy Sprague Dawley rats as well as DOCA salt hypertensive rats. By comparing spiking to prominent events in the arterial pressure curve, primarily systole and diastole, we hope to uncover mechanosensitive response in renal sensory nerves at the site of the afferent innervation to reveal what dictates ARNA. We hypothesize that afferent renal nerve activity is directly correlated to arterial pulse pressure through a mechanosensitive response. Moreover, we also

posit that this ARNA-response to arterial pressure fluctuation is impaired in DOCA-salt hypertension.

## Methods

All procedures were approved by the University of Arizona Animal Care and were in compliance with the National Institutes of Health Guide for Care and Use of Laboratory Animals.

### Animals

Male Sprague Dawley rats were purchased from Envigo (Indianapolis, IN) and given water/food in our temperature/light-controlled animal care facilities. Animals were aged to 10 weeks until the day of the nerve recording. DOCA rat preparation is listed below.

### Afferent Renal Nerve Recording

Experiments were conducted on male Sprague Dawley rats (Age: 10-12 weeks). Afferent renal nerve activity was measured in a method similar to procedures outlined in Gauthier, 2022 and Banek, 2016. Multiunit nerve recordings were performed under urethane (1800 mg/kg/h, IV) after instrumentation and isolation of a renal nerve bundle. After induction, arterial pressure (AP) is directly acquired by a left femoral artery catheter. After, the renal artery as well as corresponding nerve bundles are then revealed with an abdominal incision. A bipolar tungsten electrode is placed under the nerve bundle and encased in silicone to ensure good contact. Signal is passed through a Grass p55 preamplifier with 10x amplification (Astro-Med Inc.), a high cutoff frequency of 10 kHz, and low cutoff frequency of 1 kHz. After approximately 5 minutes

on urethane, the proximal side of the nerve bundle is surgically cut to solely measure the afferent renal nerve activity (ARNA). After 5-10 minutes of ARNA recording, the distal side is then isolated to measure electrical noise from artifacts (primarily breathing, movement). Data was acquired at a rate of 40 kHz on LabChart software (ADInstruments) and applied an optimal digital IIR filter of 60-3000 Hz. This filter was determined empirically based on the comparing Fourier transforms of pre- and post-distal sectioning signals (signal vs. noise).

Experiment 1: Healthy SD rats and the temporal structure of afferent renal nerve (ARN) spiking

Data from LabChart is imported into Spike2 (Cambridge Electronic Design) to identify spikes within ARNA. Templates are constructed for .5ms pre-trigger interval and $7\mu V$ positive threshold. Spike templates are then evaluated on a scale of 1-5 where 5 is a perfect spike template, and only templates ranking 4 or above are totaled. Spike times as well as arterial pressure data (AP) are then imported into MATLAB 2022b (The MathWorks, Inc). Within MATLAB, systole, diastole, and spike times are extracted and correlated. Spikes within 200ms (approximately 2 full cardiac cycles) of systole and diastole are compiled over all cardiac cycles within the ARNA recording, and then spike count is normalized to the total amount of cycles. This will be displayed in the form of a peri-stimulus time histogram (PSTH) where the stimulus is either systole or diastole. Then, the spike and AP results will be processed through 2 different algorithms to see clarify the relationship between renal nerve spiking and the AP trace. In the first function, spike rate is correlated to the subsequent arterial pressure value from Labchart at that instant. Finally, utilizing a frequency estimation function created by Seibold (2023), the

PSTH data is zero-padded, and the most prominent frequency is estimated and documented for each animal. A diagram showing algorithm processing is shown below:

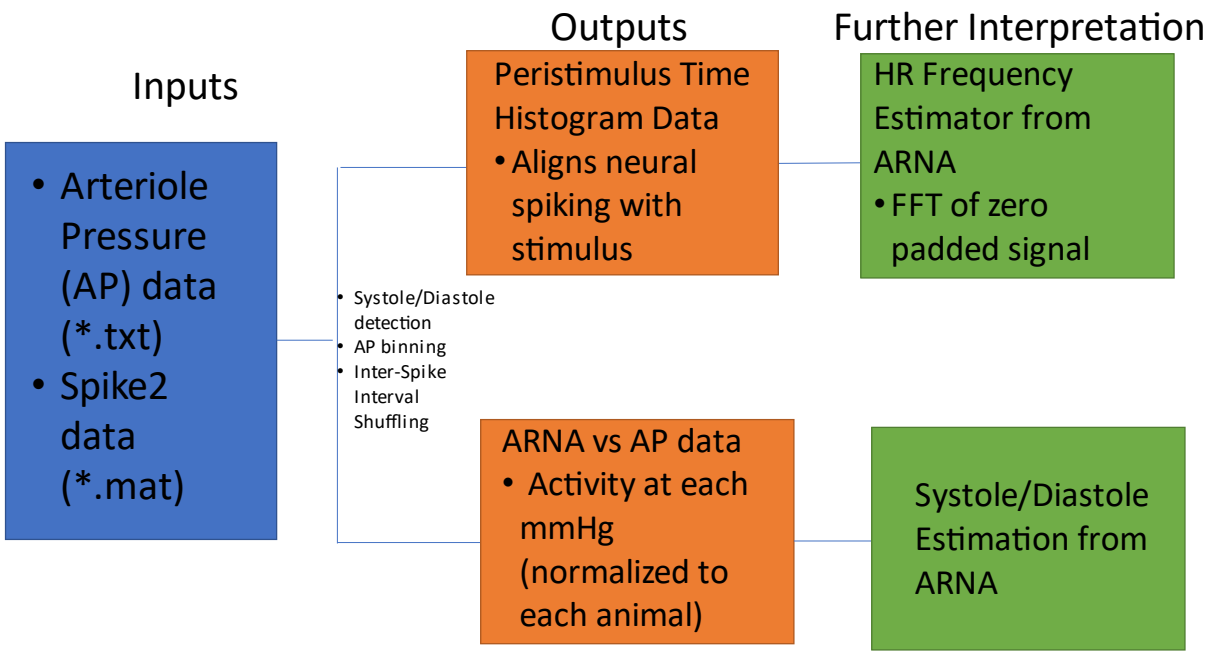


Figure 1. This flowchart shows the MATLAB algorithm steps to processing the ARNA spike train, showing the input files and formats as well as all the possible outputs depending on which algorithm is used.

All MATLAB functions will be made available on GitHub after approval of thesis committee.

Experiment 2: DOCA salt hypertensive rats and temporal ARN spiking structure

We also wanted to test for the same relationship between afferent renal nerve firing in a diseased model of animals where we know afferent nerves have an essential role in progression. In Banek Et al., 2016, this work on deoxycorticosterone acetate (DOCA) salt hypertension and ARNA, afferent activity was notably elevated in the DOCA model. To uncover the role of afferent renal spikes, 4 male SD rats were implanted with 100mg DOCA subcutaneously and given 21 days to recover. During this time, rats are given 0.9% saline and the nerve recording surgery described above would take place on the 21$^{st}$ day after implant. Data is acquired and processed exactly as described in experiment 1 to evaluate changes in the DOCA salt hypertension model.

Experiment 3: Spike cutting during low SNA periods

While the term ARNA in prior setups involved mechanical, surgical isolation of afferent signal from an intact renal nerve, the goal of this analysis involves analyzing afferent signal from a complete, intact renal nerve. We attempted to characterize bursts utilizing the integrated signal (typical method of sympathetic burst characterization) and extracted them from the recordings to analyze times of low RSNA in attempt to solely measure ARNA from an intact nerve. This novel approach to isolation of ARNA to discriminate ARNA from RSNA utilizes the same IIR 60-3000 Hz filtered recordings (pre-afferent dissection) and are integrated In Labchart with a .025 integration constant. In MATLAB, thresholds are semi-automatically selected based on relative minima and maxima of the integrated signal. Ideally, the bottom threshold should be 1-2 standard deviations away from the average minimum, to ensure that sympathetic bursting

activity is wholly excluded from the threshold. This integrated signal is then used as a mask which is applied to the raw signal, effectively creating an artificial "low sympathetic tone" afferent renal nerve recording. Similar to prior processing, the inter-burst ARNA (ibARNA) is then spike cut in Spike2 and graphed in MATLAB. The only difference between analyses is that spike activity normalization is based on time as opposed to heart rate. Note that this analysis was only done in SD, healthy animals.

# Results

## Experiment 1: Healthy SD rats and the temporal structure of ARN spiking

Below is a representative 200 millisecond window of concurrent blood pressure and afferent renal nerve recording. All results for the PSTH graphs will be includes thousands (5 minute recording, ~1800 heartbeats) all normalized to show a temporal relationship with blood pressure.

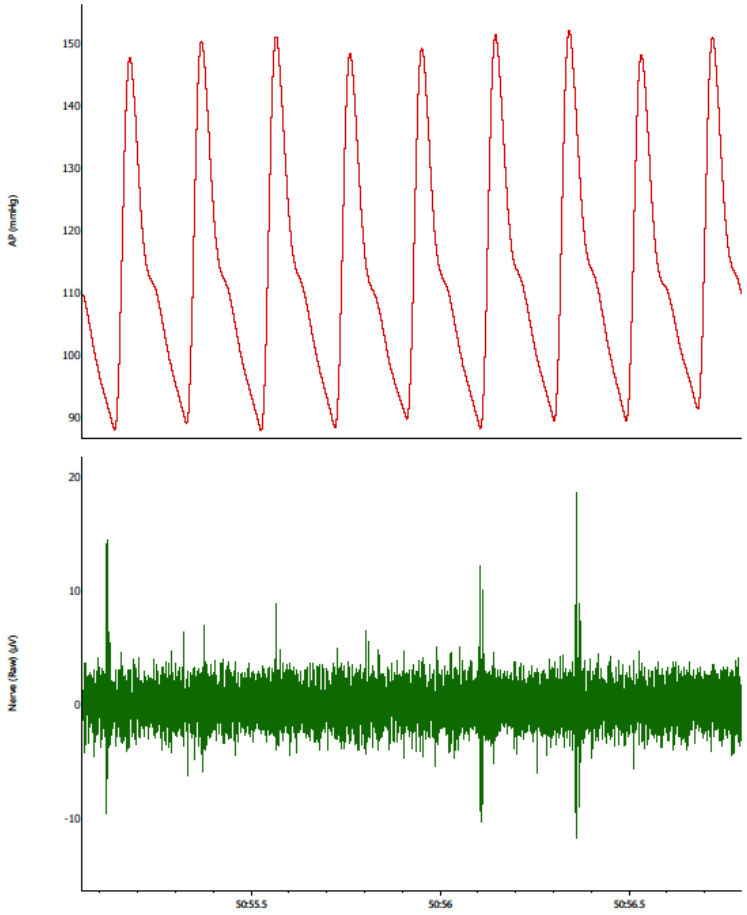


Figure 2. This figure demonstrates a sample of a subject's raw, filtered afferent renal nerve firing along with concurrent femoral arterial pressure readings.

For all healthy animals, there was a grouped afferent renal nerve response at diastole shown by the figure below when compared to each animals randomized spike train. From 10 to 0

milliseconds before diastole, afferent spiking rate was elevated at .28 ± .12 spikes per 10ms/total heartbeats compared to the randomized spike train which had a spiking rate of .13 ± .05 spikes per 10ms/total heartbeats (**P<.002 t= -.01 vs t= 0 [Diastole], Dunnett's multiple comparisons test). The average spiking rate of the randomized spike train is .14 ± .05 spikes per 10ms/total heartbeats, serving as a baseline of ARN spiking rate, as all temporal structure has been randomized. The graph correlating ARN spiking to systole demonstrates the same peak activity response at diastole, simply shifted over to demonstrate predictability of both pressure change events (spontaneous baroreflex).

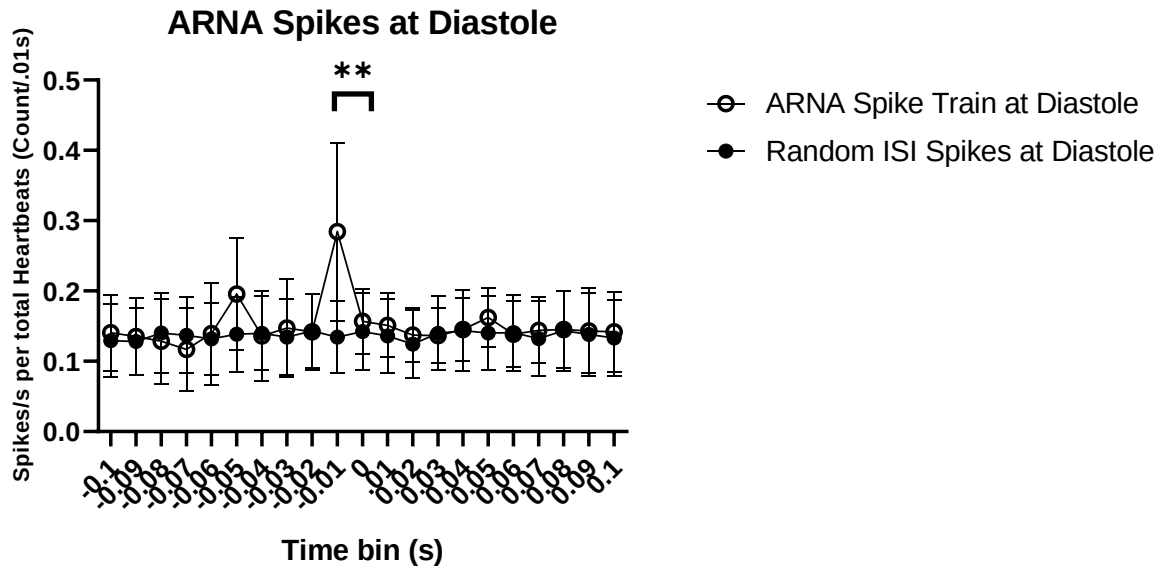
ARNA Spikes at Diastole
**
Spikes/s per total Heartbeats (Count/.01s)
0.5
0.4
0.3
0.2
0.1
0.0
-0.1
-0.09
-0.08
-0.07
-0.06
-0.05
-0.04
-0.03
-0.02
-0.01
0
0.01
0.02
0.03
0.04
0.05
0.06
0.07
0.08
0.09
0.1
Time bin (s)
ARNA Spike Train at Diastole
Random ISI Spikes at Diastole

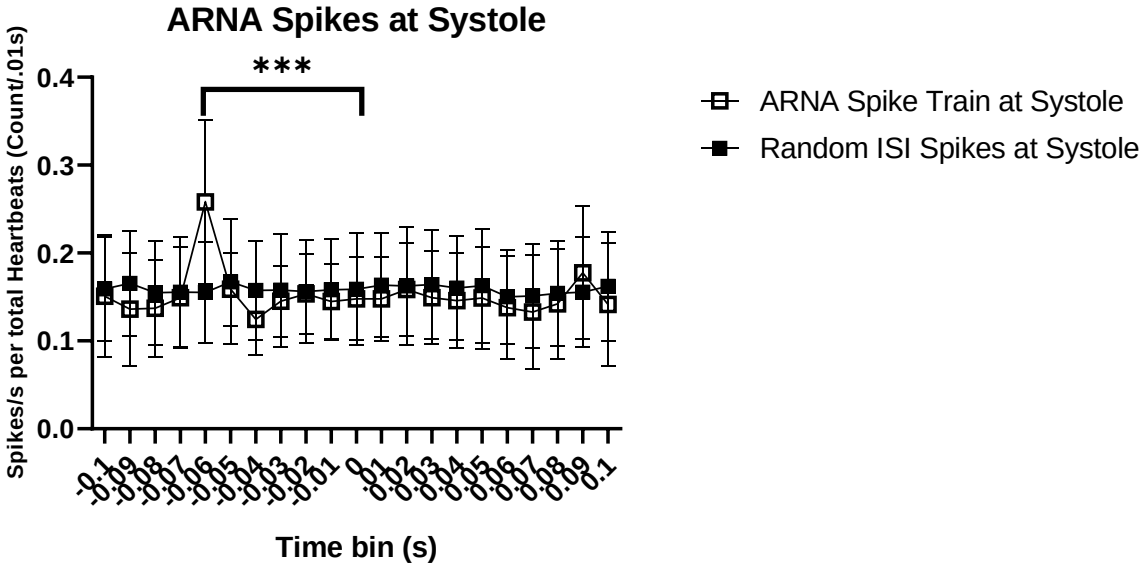
ARNA Spikes at Systole
***
Spikes/s per total Heartbeats (Count/.01s)
0.4
0.3
0.2
0.1
0.0
-0.1
-0.09
-0.08
-0.07
-0.06
-0.05
-0.04
-0.03
-0.02
-0.01
0
0.01
0.02
0.03
0.04
0.05
0.06
0.07
0.08
0.09
0.1
Time bin (s)
ARNA Spike Train at Systole
Random ISI Spikes at Systole

Figure 3. This is the representation of afferent renal nerve spiking around times of systole and diastole (represented by time zero) for a binned total 200ms window (100ms before and after stimulus). A, The renal nerve spike train in healthy animals (n=5) has heightened afferent spiking at a time .01 to 0 seconds before diastole (t = 0) when compared to baseline levels (**P<.002 t= -.01 vs t= 0 [Diastole], Dunnett's multiple comparisons test). B, The renal nerve shows a heightened rate of afferent spiking at a time -.06 to 0.05 seconds before the stimulus when compared to the same ISI shuffled spike train (***P<.001 t=-.06 vs t=0 [diastole], Dunnett's multiple comparisons test).

The figure below overlays a blood pressure trace over a singular health animal PSTH for both pressure events (each subsequent trace is time shifted to show systole/diastole), visually demonstrating the high correlation between systole and diastole. Heart rate can also be derived from the spike rate (y axis), but this is further explored in the following figures.

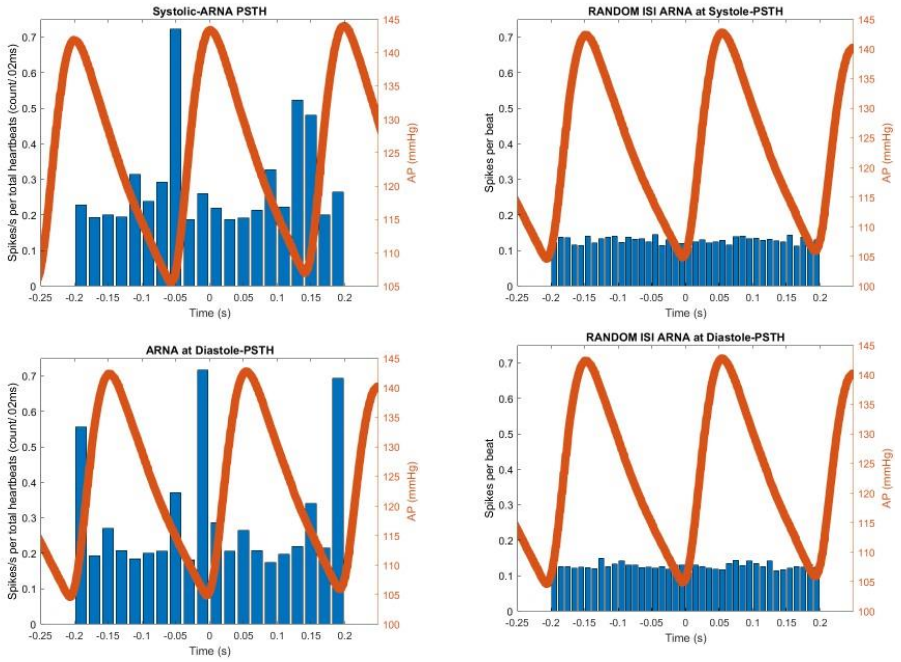


Figure 4. PSTH graphs for an individual animal overlayed with arterial pressure. A, Given the previous results, the significant time at -.06 to -.05 seconds seems to correlate with diastole of the arterial pressure curve. This will be further evaluated in the following figures. B, With no significance between bins, there is no relationship between the random spikes group and arterial pressure. C, From -.01 to 0 seconds, arterial pressure is related to afferent renal nerve spiking. D. similar to B, there is no relationship between random ISI spikes at the time of diastole.

Next, to see the spiking rate for an entire trace, for 1 animal, these two graphs show intermediary compilation of firing rate at each blood pressure point within a given trace to see if

certain pressures were favored. The typical trace on the left featured two relative maxima while a rarer trace on the right featured a third hump at an intermediary pressure.

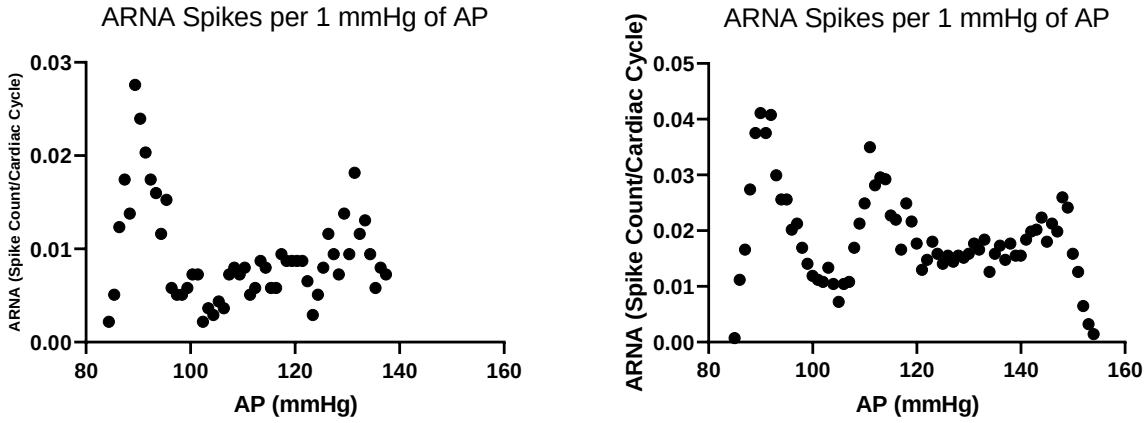


Figure 5. These two graphs plot afferent renal spiking activity at each measured blood pressure value for each animal. A, This animal has 2 arterial pressure events of interest, which will be related in the next section. B, This animal has 3 particular arterial pressures where afferent activity is elevated.

Using the location of the relative maxima from the graph above (pressures where spiking rate peaks), we see that there is a high predictability of pressures at which ARNA is spiking the most with both systole and diastole, further reinforcing the predictive capability of this relationship (A: ***P<.0001, linear correlation, $R^2$=.9965, B: ***P<.0008, linear correlation, $R^2$=.9854).

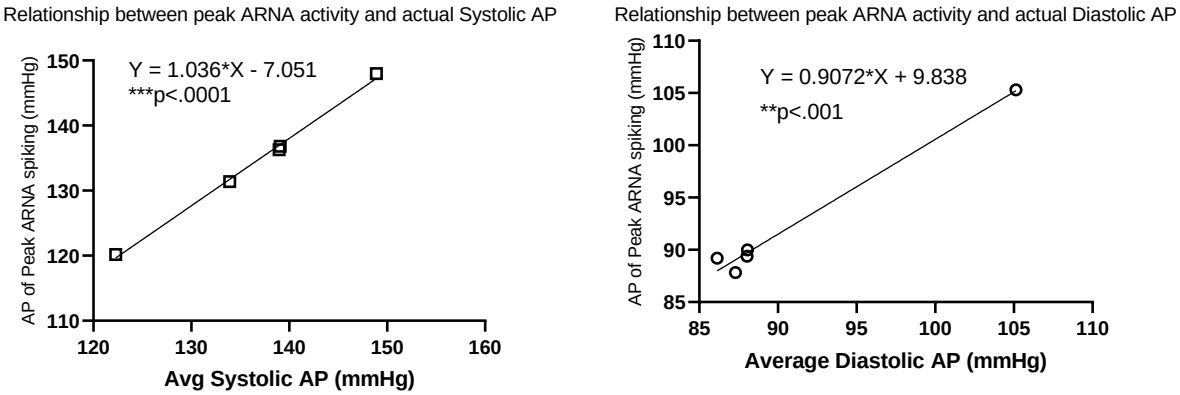


Figure 6. A, Peak neural activity blood pressures from figure 3 were compiled at the high end (>120 mmHg) and compared to average systole over the same time period in Labchart. The linear slope is significantly non-zero (***P<.0001, linear correlation, $R^2$=.9965). B, Peak neural activity blood pressures from figure 3 were compiled at the low end (<110 mmHg) and compared to average diastole over the same time period in Labchart. The slope is also significantly non-zero (***P<.0008, linear correlation, $R^2$=.9854).

Finally, evaluating spiking rate for an extended window of systole and diastole, we also observed a high correlation of being able to extract heart rate from looking at the rate of afferent renal nerve spiking for each animal and guessing the frequency using a frequency estimation algorithm (Systole: ***P<.0004, linear correlation, $R^2$=.9897, Diastole: *P<.05, linear correlation, $R^2$=.87). There was no relationship for the random ISI spike train as expected.

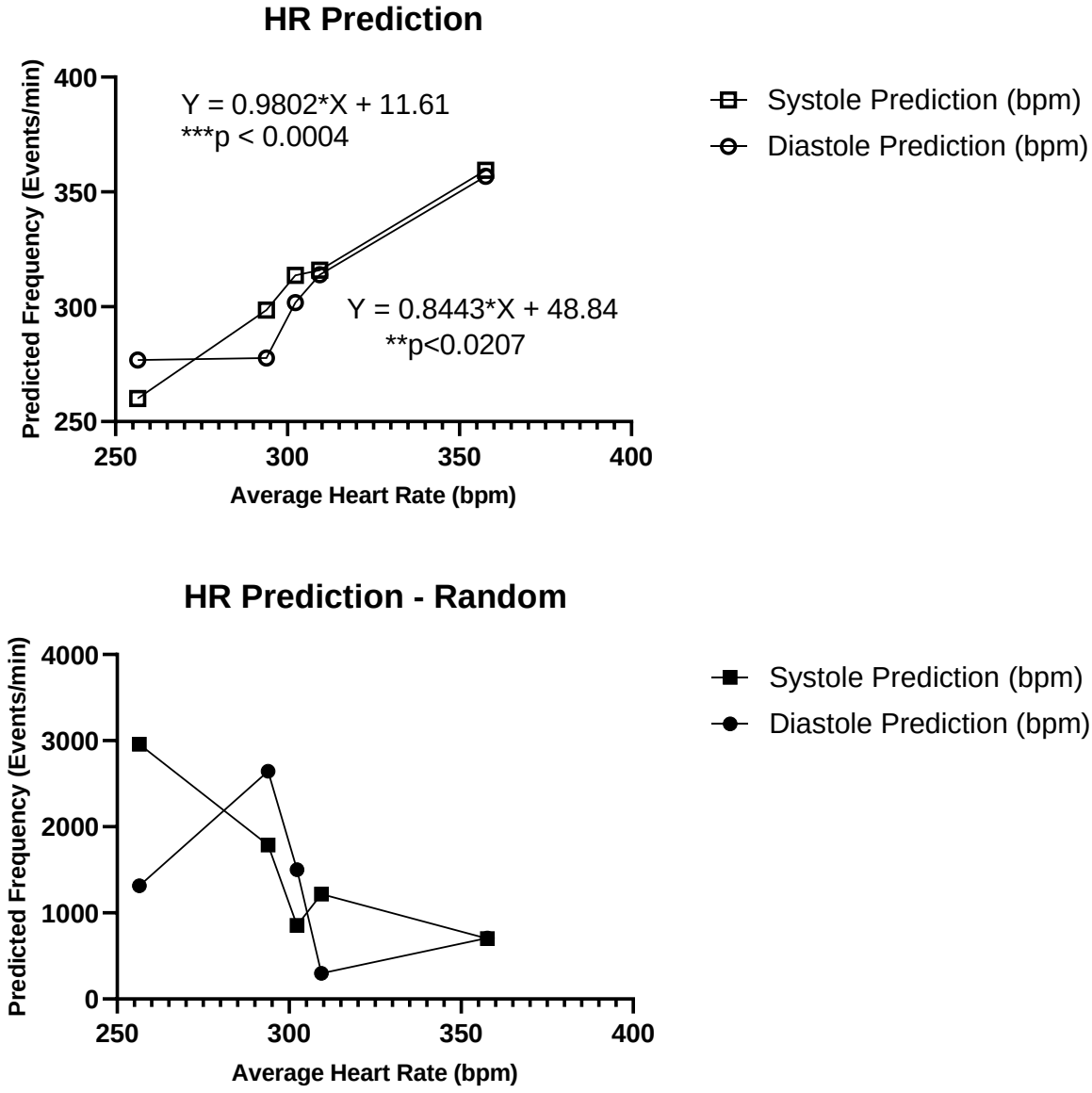


Figure 7. A, Frequency estimation (from FFT of afferent renal spiking of figure 1/2) correlated with the actual heart rate of the animal from time of recording (Labchart). Both the slope of the systole and diastole estimations are significantly non-zero (Systole: ***P<.0004, linear

correlation, $R^2$=.9897, Diastole: *P<.05, linear correlation, $R^2$=.87). B, This is the same graph, however, displaying the randomized ISI spike train for systole and diastole. Both curves have a non-significant non-zero slope (Systole: ns, linear correlation, $R^2$=.7570, Diastole: ns, linear correlation, $R^2$=.5069)

Experiment 2: DOCA salt hypertensive rats and temporal ARN spiking structure

In the DOCA group, there were no significant relationships at diastole. However, similar to the normalization above, by comparing afferent activation to the minimum .33 ± .20 spikes per 10ms/total heartbeats, which in this case occurs from 80 to 70 milliseconds before diastole, there was heightened activity at 50 to 40 milliseconds (.54 ± .24 spikes per 10ms/total heartbeats) before and 20-30 milliseconds (.49 ± .34 spikes per 10ms/total heartbeats) after diastole. We also note that average ISI shuffled spike rate is 0.43 ± .26 spikes per 10ms/total heartbeats which is elevated compared to the normotensive group, but activity at the two times of elevated activity were only slightly higher than baseline levels in comparison with the two-fold response in the healthy group.

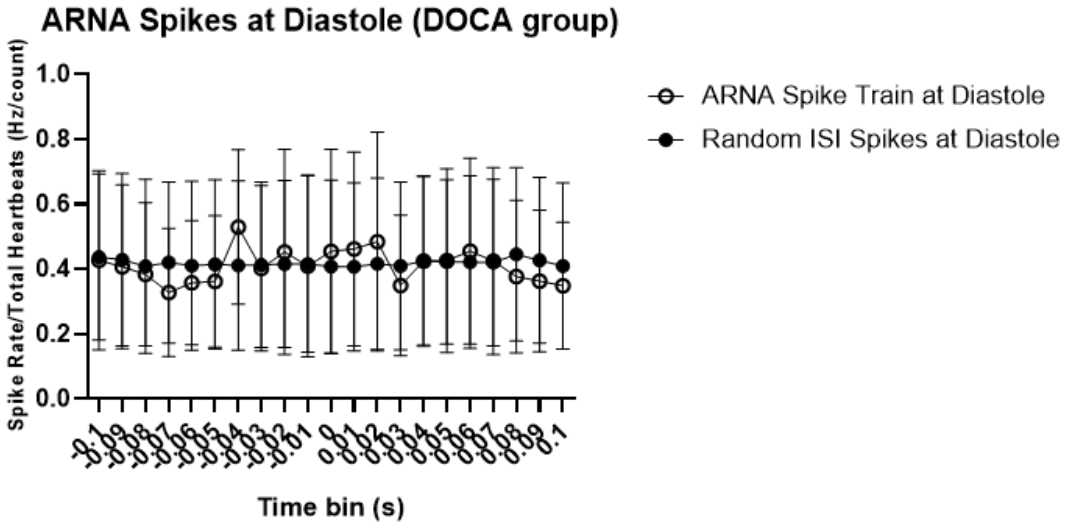


Figure 8. Afferent renal nerve PSTH in hypertensive DOCA salt animal group. Compared to 80 to 70 milliseconds before diastole, there is elevated afferent spiking at 50 to 40 milliseconds before diastole and 20-30 milliseconds after diastole (**P<.002 t=-.07 vs t= .04, and *P<.02 t=-.07 vs t= .02, Dunnett's multiple comparisons test).

Experiment 3: Spike cutting during low SNA periods

This spike train was cut from healthy, sympathetic, total renal nerve recordings and manually thresholded to exclude sympathetic bursting activity. This spike train shows no relationship near diastole; however, there is a significant change in spike rate when using minimum activity at around 40-30 milliseconds before diastole as a baseline. Compared to 40-30

milliseconds before diastole (.65 ± .47 spikes per $s^2$), the activity for each bin from 30-40, 40-50, and 50-60 milliseconds is 3.9 ± 5.3 spikes per $s^2$, 4.5 ± 7.1 spikes per $s^2$, and 3.9 ± 6.0 spikes per $s^2$, respectively. We also qualitatively noted that this inter-burst spiking activity at diastole seems to be more periodic than the previous relationship.

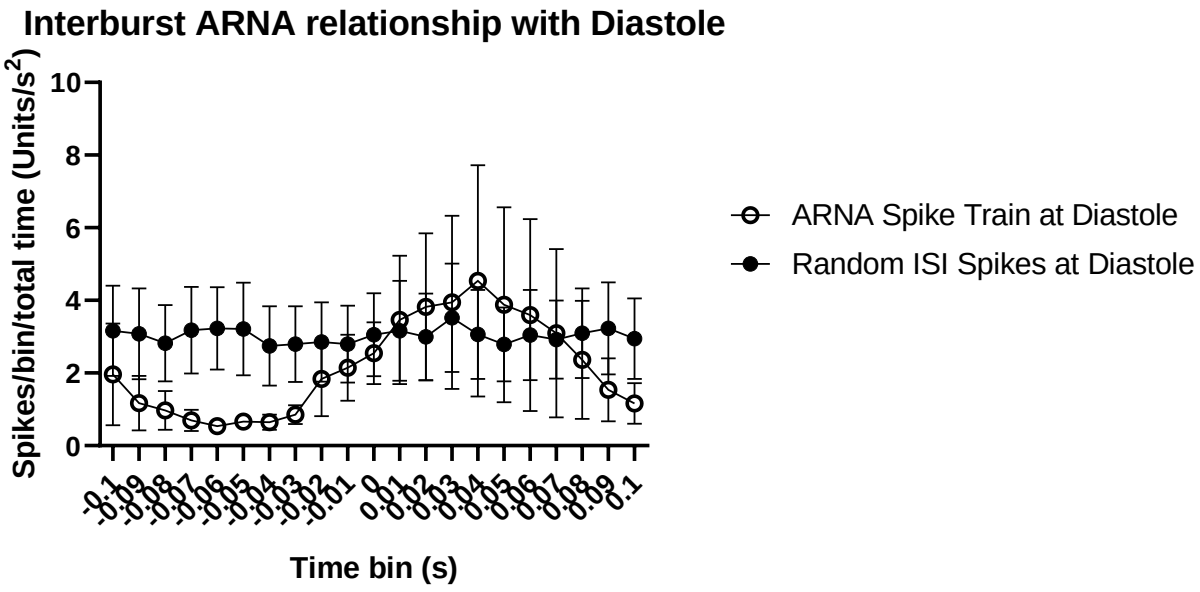


Figure 9. After semi-automatically excluding sympathetic bursts, this figure shows the subsequent spike train in a PSTH where the trigger is diastole. While there is no relationship at time t=0 (diastole), there is a significant different between the minimum and maximum spiking (t=-.04 vs t=.03, .04, and .05) (*P<.05 t=.03, .04, and .05 vs t=0 [diastole], Dunnett's multiple comparisons test).

Spike Verification

Spike quality is an important factor in the collection of ARN spikes. Due to the nature of these extracellular recordings, multiunit recordings were necessary due to the unknown number of axons in each isolated renal nerve bundle. As mentioned above, template rating was one measure in which quality was controlled between trials. Below are sample traces of spike cutting for healthy and DOCA hypertensive nerve recordings to visually show efficacy in consistency of the shapes of these waveforms.

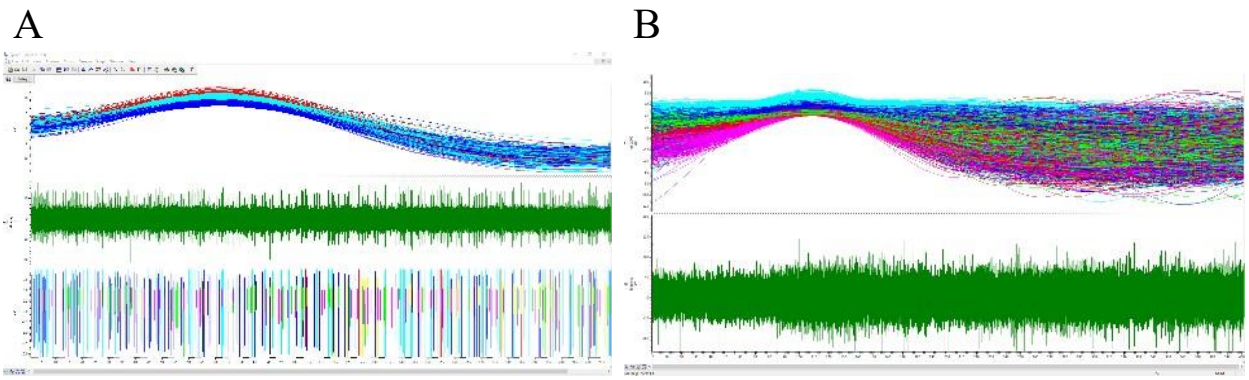


Figure 10. These are two sample traces of filtered afferent renal nerve recordings addressing studies 1 and 2. A, Waveform of all spikes throughout the entire recording of a healthy Sprague Dawley animal are shown in channel 1 on top. Channel 2 shows the filtered, raw recording and 3

demonstrates the time of each wave mark. Note the clear depolarization, repolarization, as well as beginning of the hyperpolarization. B, This screenshot shows the total waveforms for the DOCA hypertensive group in channel 1 while the raw is in channel 2. Note that while depolarization and repolarization are consistent for each template, hyperpolarization is a lot noisier, which could be due to elevated noise in these diseased states.

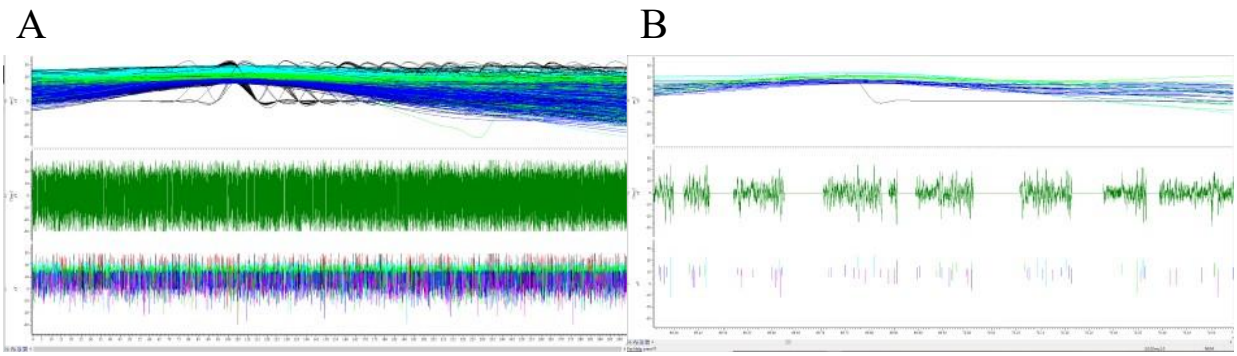


Figure 11. Waveform of spikes extracted from the thresholded total RSNA recording of Afferent Spikes. A. Similar to the prior figure, channel one demonstrates all waveforms showing a very consistent depolarization and repolarization for these selected spikes. Channel 2 is an example of a thresholded RSNA filtered, raw recording. Channel three shows times of wavemarks. Note: I wanted to include the black spike template which is artificially labeled as noise (these were

excluded from the previous figure). By showing the noise spikes, we wanted to exemplify that these strict numerical thresholds may interfere with pattern recognition in Spike2, causing these false positives; however, spotting them is simple due to the stark drops to 0 microvolts which are indicative of these artificially altered, noise patterns. B, This screenshot shows the same as A, but zoomed in to show the locations of these bursts which have been completely extracted from the total nerve signal to only highlight afferent control. The signal in B is visually comparable to an afferent renal nerve recording (compare to figure 9, A)

## Discussion

As seen in experiment 1, healthy normotensive animals showed an overall trend of increased spiking at diastole. To our knowledge, this is the first evidence of the mechanism of cardiovascular modulation from afferent renal nerves on a beat-to-beat basis, independent of sympathetic stimulation. One of the first papers that discuss mechanoreceptor activity in the kidney was conducted by the Niijima et al. group in 1971. Their work was done in a perfused kidney where pressure was artificially modulated by approximately 50mmHg across the renal artery, increasing afferent renal nerve spiking. While these results complement our findings with the DOCA salt hypertensive group result of elevated tonic, baseline spike rate, our findings clearly highlight the temporal structure of the spike train with regards to the cardiac cycle. Understanding when these ARN spiking events occur with relation to the cardiac cycle strengthens understanding of the role of afferent renal nerves as responding to pressure related events (systole and diastole) in the arterial walls.

Notably, though, sensory nerve firing peaks at diastole, where arterial pressure is low. While carotid baroreceptors are activated by arterial stretch, mechanoreceptors in the kidney seem to be demonstrating the opposite behavior. Our group speculates that these mechanoreceptors could be responding to changes, (specifically drops) in pressure as opposed to stretching. We expect these sensory nerves to be located near the renal artery or arterioles, to sense these large changes in arterial pressure from pumping of the heart.

This pattern in afferent renal nerve firing also may also have implication in the field/understanding of renal denervation. In the SPYLAR hypertension trials of a method of catheter denervation to ablate nerves, though rare, a very small percentage of patients saw an increase in SBP over time (Bhatt, et al, 2014). While previous reviews argued decreased RSNA activity prior to the denervation, these results support the idea that ablation of the afferent nerves may also be contributing to this deregulation of the cardiac cycle.

Consistent firing that only occurs at diastole could be evidence of renal nerve electroceutical activity, modulating large changes in blood pressure such as elevated SBP (from i.e. renal damage, sodium retention, elevated activity of the renin angiotensin aldosterone system). Reviews such as Veiga et al., 2021 argue that looking at the roles of afferent nerves, particularly in denervation could improve efficacy of renal denervation.

In experiment 2, the DOCA hypertensive group had no significance when related to these pressure changing events but showed elevated activity when compared to minimum firing at 70 milliseconds before diastole. Failing to detect afferent spiking at diastole in DOCA animals compared to SD controls provides insight to afferent renal nerve control in DOCA hypertension model. First, the temporal structure in DOCA animals is eliminated. Since we could not detect a difference at diastole, ARN firing times may be active at different times in the cardiac cycle which is show by this elevated activity when compared to the animals minimum spiking frequency activity. We suspect that damage from hypertension may play a role in these mechanoreceptors' role to spike at the same time in the cardiac cycle as the healthy animals.

Secondly, since both the healthy and hypertensive firing rates are normalized to total heartbeats, the total frequency of firing can also be compared between the two groups. As mentioned in the results for the DOCA group firing rate, healthy animals had a greater difference in elevated versus baseline firing rate compared to the DOCA animals which had a relatively smaller difference between peak spiking and baseline rate. These results not only support the 2016 Banek findings of elevated afferent renal nerve activity in DOCA, in this case shown by ARN spiking, but also support ideas that elevated baseline tone is what is causes renal dysfunction. In addition to temporal breakdown, our group argues that in DOCA salt hypertension, the masking of these mechanoreceptor spikes by other afferent renal nerve basal activity (sensory nociceptor activity, sympathetic feedback, salt natriuresis, or any other afferent renal nerve role) may be a contributor to the end stage cardiac dysfunction.

By trying to analyze afferent tone within sympathetic bursts in experiment 3, the relationship at diastole (t=0) is not detected. Though we acknowledge that spiking frequency cannot be directly compared as is in experiments 2 and 3 due to the lack of heartbeat normalization, analyzing spike frequency shifts across each spike train's x-axis at the stimulus of diastole allows for analysis of spike train temporal structure. A time-shift occurs when comparing the minimum and maximum firing (40ms before and after diastole), showing some sort of modulation by the fact these nerves are intact, meaning that sympathetic nerves may have some effect on afferent signaling. In our case, we speculate that intact sympathetic nerves are modulating or altering the firing rate to maximal firing after mechanosensory input. Our results support findings in Kopp, 2007 work demonstrating that efferent signal increases afferent nerve

firing by norepinephrine activation of α-adrenoceptors. Norepinephrine release from sympathetic burst firing may be altering time of sensory firing (time shifting ARNA spikes away from diastole) initiating an efferent-afferent modulation that dictates known cardiovascular control in the kidney. This explanation is consistent with the physiological significance of elevating sympathetic control systemically (and quickly) in the body (fight or flight). However, it must be noticed that by normalizing the afferent spiking rate to its own minimum, significant structure can be detected by the inter-burst spiking, but the relation is devoid of feedback from features of the arterial pressure waveform.

Though, it must also be noted that these results only support the renorenal hypothesis partially. As seen in the effects of studies one and two, our results still support the idea of elevated afferent renal nerve activity in disease as opposed to a decrease in afferent spiking for arterial pressure maintenance.

Our group also wanted to distinguish and differentiate electrocardiogram (EKG) signal from the renal nerve spiking recordings since both occur at similar times in the cardiac cycle. The afferent renal spikes are not artifacts of EKG because of afferent spiking rates occurring at 25 to 30 percent of total heartbeats as opposed to EKG which would have a rate of 100 percent. Additionally, waveforms do not typically include P and T waves which are indicative of EKG.

Overall, these results have implications on improving the understanding of the role of afferent renal nerve activity in healthy as well as diseased hypertensive animals, as well as possible capabilities of longitudinal studies outlined by aim 3 of inter-burst RSNA cutting. Particularly in the scope of renal denervation treatment, understanding when ARNA events are

occurring can provide more insight into bettering denervation efficacy as well as personalized treatment (patients option of total versus sympathetic versus afferent renal nerve ablation). With the advancement of recording RSNA with radio-telemeters, along with possible improvements to the thresholding in total recording to take a spectral approach, longitudinal afferent recording could be possible soon.

Future steps for this project could include immunohistochemistry in vivo to evaluate the location of these mechanoreceptors and labeling of neurotransmitters to study how action potentials are being fired at arterial stretch (diastole). Labeling of the central nervous system (CNS), in particular the brain, in vivo could also be imaged in concurrence with arterial pressure recordings to see if these same action potentials are occurring/detectable within the CNS.

References

Burke, S. L., & Head, G. A. (2003). Method for in vivo calibration of renal sympathetic nerve activity in rabbits. Journal of Neuroscience Methods, 127(1), 63–74. https://doi.org/10.1016/S0165-0270(03)00121-3

Feng, N.-H., Lee, H.-H., Shiang, J.-C., & Ma, M.-C. (2008). Transient receptor potential vanilloid type 1 channels act as mechanoreceptors and cause substance P release and sensory activation in rat kidneys. American Journal of Physiology-Renal Physiology, 294(2), F316–F325. https://doi.org/10.1152/ajprenal.00308.2007

Frame, A. and Wainford, R. (2017), The role of the mechanosensitive renal sensory afferent nerve sympathoinhibitory reno-renal reflex in sympathetic outflow, natriuresis, and blood pressure regulation. The FASEB Journal, 31: 718.8-718.8. https://doi.org/10.1096/fasebj.31.1_supplement.718.8

Katsurada, K., Shinohara, K., Aoki, J., Nanto, S., & Kario, K. (2022). Renal denervation: basic and clinical evidence. Hypertension Research, 45(2), 198–209. https://doi.org/10.1038/s41440-021-00827-7

Kopp, U. C., Cicha, M. Z., Smith, L. A., Mulder, J., & Hökfelt, T. (2007). Renal sympathetic nerve activity modulates afferent renal nerve activity by PGE2-dependent activation of α1- and

α2-adrenoceptors on renal sensory nerve fibers. American Journal of Physiology-Regulatory, Integrative and Comparative Physiology, 293(4), R1561–R1572. https://doi.org/10.1152/ajpregu.00485.2007

Kopp, U. C. (2015). Role of renal sensory nerves in physiological and pathophysiological conditions. American Journal of Physiology - Regulatory, Integrative and Comparative Physiology, 308(2), R79–R95. https://doi.org/10.1152/ajpregu.00351.2014

Lohmeier, T. E., Hildebrandt, D. A., Warren, S., May, P. J., & Cunningham, J. T. (2005). Recent insights into the interactions between the baroreflex and the kidneys in hypertension. American Journal of Physiology-Regulatory, Integrative and Comparative Physiology, 288(4), R828–R836. https://doi.org/10.1152/ajpregu.00591.2004

Matsushita, K., Ballew, S. H., Wang, A. Y.-M., Kalyesubula, R., Schaeffner, E., & Agarwal, R. (2022). Epidemiology and risk of cardiovascular disease in populations with chronic kidney disease. Nature Reviews Nephrology, 18(11), 696–707. https://doi.org/10.1038/s41581-022-00616-6

Nishi, E. E., Martins, B. S., Milanez, M. I. O., Lopes, N. R., de Melo, J. F., Pontes, R. B., Girardi, A. C., Campos, R. R., & Bergamaschi, C. T. (2017). Stimulation of renal afferent fibers

leads to activation of catecholaminergic and non-catecholaminergic neurons in the medulla oblongata. Autonomic Neuroscience, 204, 48–56. https://doi.org/10.1016/j.autneu.2017.01.003

Osborn, J. W. (2005). HYPOTHESIS: SET-POINTS and LONG-TERM CONTROL OF ARTERIAL PRESSURE. A THEORETICAL ARGUMENT FOR A LONG-TERM ARTERIAL PRESSURE CONTROL SYSTEM IN THE BRAIN RATHER THAN THE KIDNEY. Clinical and Experimental Pharmacology and Physiology, 32(5-6), 384–393. https://doi.org/10.1111/j.1440-1681.2005.04200.x

Osborn, J. W., Tyshynsky, R., & Vulchanova, L. (2021). Function of Renal Nerves in Kidney Physiology and Pathophysiology. Annual Review of Physiology, 83(1), 429–450. https://doi.org/10.1146/annurev-physiol-031620-091656

Ott, C., Mahfoud, F., Mancia, G., Narkiewicz, K., Ruilope, L. M., Fahy, M., Schlaich, M. P., Böhm, M., & Schmieder, R. E. (2021). Renal denervation in patients with versus without chronic kidney disease: results from the Global SYMPLICITY Registry with follow-up data of 3 years. Nephrology Dialysis Transplantation, 37(2), 304–310. https://doi.org/10.1093/ndt/gfab154

Sata, Y., Head, G. A., Denton, K., May, C. N., & Schlaich, M. P. (2018). Role of the Sympathetic Nervous System and Its Modulation in Renal Hypertension. Frontiers in Medicine, 5(82). https://doi.org/10.3389/fmed.2018.00082

Seibold, Peter (2023). Sine fitting (https://www.mathworks.com/matlabcentral/fileexchange/66793-sine-fitting), MATLAB Central File Exchange. Retrieved April 19, 2023.

Veiga, A. C., Milanez, M. I. O., Campos, R. R., Bergamaschi, C. T., & Nishi, E. E. (2021). The involvement of renal afferents in the maintenance of cardiorenal diseases. American Journal of Physiology-Regulatory, Integrative and Comparative Physiology, 320(1), R88–R93. https://doi.org/10.1152/ajpregu.00225.2020

Wadei, H. M., & Textor, S. C. (2012). The role of the kidney in regulating arterial blood pressure. Nature Reviews Nephrology, 8(10), 602–609. https://doi.org/10.1038/nrneph.2012.191

Xu, B., Zheng, H., Liu, X., & Patel, K. P. (2015). Activation of afferent renal nerves modulates RVLM-projecting PVN neurons. American Journal of Physiology-Heart and Circulatory Physiology, 308(9), H1103–H1111. https://doi.org/10.1152/ajpheart.00862.2014